Volume 55 | Number 27 | 7 April 2019 | Pages 3841–3992

ChemComm

Chemical Communications

rsc.li/chemcomm

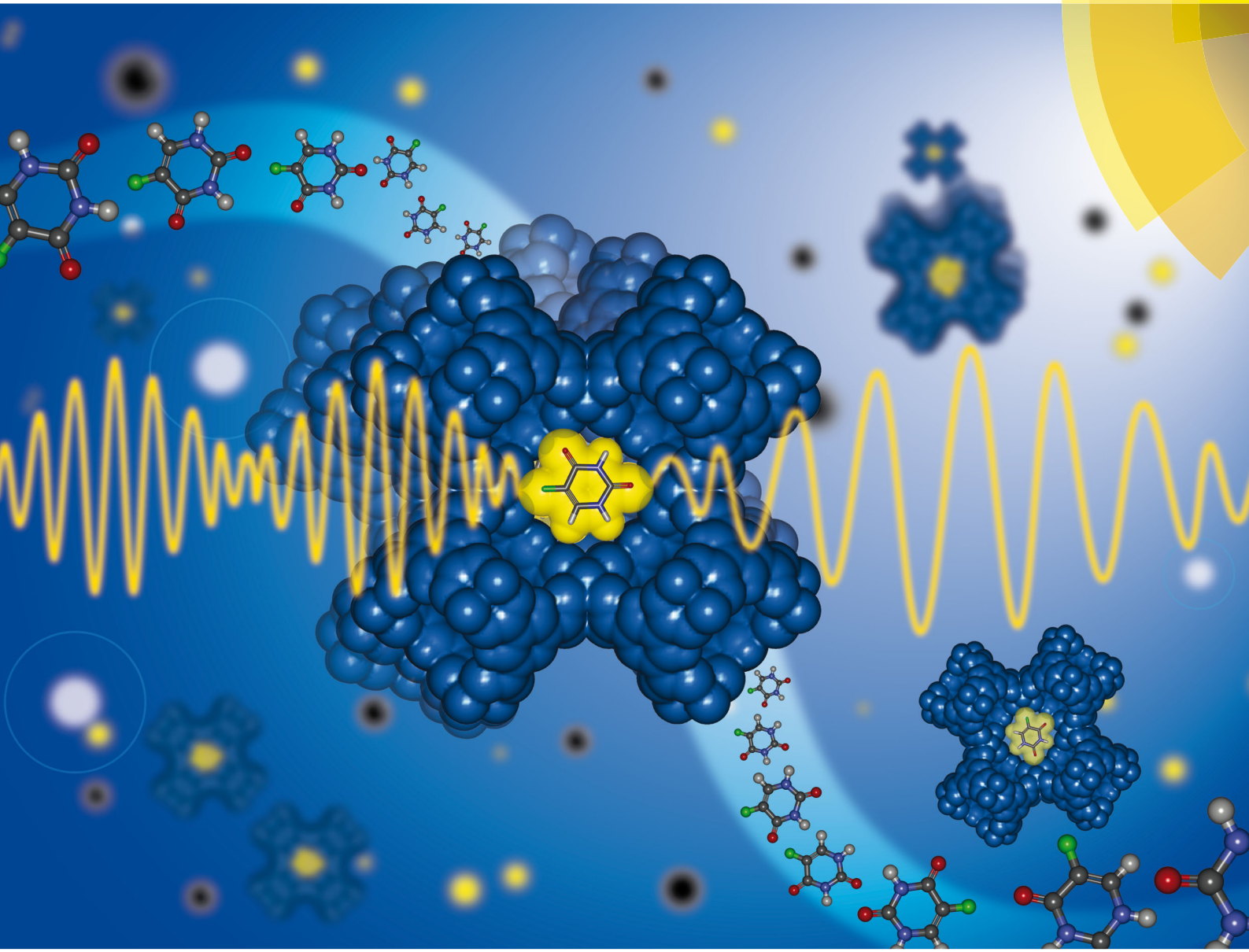

ISSN 1359-7345

ROYAL SOCIETY OF CHEMISTRY | Celebrating IYPT 2019

COMMUNICATION

Jin-Chong Tan *et al.*

Guest–host interactions of nanoconfined anti-cancer drug in metal–organic framework exposed by terahertz dynamics

ChemComm

COMMUNICATION

Cite this: *Chem. Commun.*, 2019, **55**, 3868

Received 20th December 2018,
Accepted 18th February 2019

DOI: 10.1039/c8cc10089f

rsc.li/chemcomm

Guest–host interactions of nanoconfined anti-cancer drug in metal–organic framework exposed by terahertz dynamics†

Barbara E. Souza,[a] Svemir Rudić,[b] Kirill Titov,[a] Arun S. Babal,[a] James D. Taylor[b] and Jin-Chong Tan *[a]

A facile mechanochemical method was employed to accomplish one-pot encapsulation of anti-cancer drug 5-fluorouracil (5-FU as guest) in a metal–organic framework (HKUST-1 as host). Vibrational spectroscopy *via* inelastic neutron scattering was applied to probe guest–host interactions arising from nanoscale confinement. We compare 5-FU@HKUST-1 derived from *in situ* and *ex situ* encapsulation.

Metal–organic frameworks (MOFs) are emergent multifunctional materials that have garnered considerable attention in the last decade. The copper-based framework termed HKUST-1 [$Cu_3(BTC)_2$; BTC = benzene-1,3,5-tricarboxylate] has been explored as a viable host for the creation of bio-oriented guest@MOF composite systems.[1] Notably, the coordinatively unsaturated metal sites (CUS) in the pores of HKUST-1 are highly accessible, which may act as a strong binding site for guest drug molecules.[2] There has also been a rising interest in the development of biologically and environmentally friendly synthesis methods to yield porous frameworks. For instance, the development of facile mechanochemical techniques for preparing MOFs may help to mitigate the use of toxic and costly organic solvents.[3]

Various studies have reported the use of mechanochemistry for the synthesis of HKUST-1, where ball milling has been used to accomplish neat or liquid-assisted grinding to fabricate porous frameworks.[4] However, one-pot encapsulation of guest molecules into MOFs *via* mechanochemistry is less common, especially its comparison with post-synthetic encapsulation, has not yet been investigated in detail. While the chemical structure and encapsulation of certain drug@MOF combinations (guest@host system) have been published,[6] to the best of our knowledge there is no study interrogating the interactions between the (guest) drug molecules and the (host) framework *via* lattice dynamics. An improved understanding of guest–host interactions will be central to establishing pathways to control the binding/release of drug molecules from MOFs as carriers.[7]

Inelastic neutron scattering (INS) is a powerful spectroscopic technique based on the scattering of neutrons by the nuclei of condensed matter. Unlike optical spectroscopic techniques (*e.g.* infrared or Raman), INS is not subject to optical selection rules, therefore all transitions are active in INS spectra.[8] The neutron is a highly sensitive probe to measure local changes in vibrational modes (low energy phonons and higher frequency molecular vibrations), and their associated intensities as a test of intermolecular forces. INS is the ideal technique to probe the molecular vibrations where the guest molecule is bound either in a crystal or adsorbed on the surface.[9]

In this work, we report the detailed characterization of drug@MOF systems *via* INS as recorded on the TOSCA neutron spectrometer.[10] We utilize a mechanochemical method (manual grinding) to accomplish *in situ* encapsulation of the anti-cancer drug: 5-fluorouracil (5-FU), within the HKUST-1 host framework, yielding the 5-FU@HKUST-1_IN composite. We demonstrate its feasibility as a facile one-pot self-assembly strategy, in contrast to the *ex situ* encapsulation method to yield 5-FU@HKUST-1_EX (*via* immersion of pre-activated host in a saturated drug solution); the former has the potential to minimize the "burst effect",[11] which is an outstanding limitation to the practical use of many porous host structures as drug carriers. Details of the synthetic routes are presented in the ESI.†

Fig. 1a illustrates the possible guest–host interaction of 5-FU with the CUS located on the copper paddle-wheel of HKUST-1, forming C–F···Cu or C═O···Cu coordination. Indeed, similar interactions involving organic molecules binding to HKUST-1[2b,12] and other MOFs with open metal centres have been reported.[13] Fig. 1b shows the powder X-ray diffraction (PXRD) patterns of the activated samples, confirming the successful synthesis of crystalline HKUST-1 through mechanochemistry. While the

[a] *Multifunctional Materials and Composites (MMC) Laboratory, Department of Engineering Science, University of Oxford, Parks Road, Oxford, OX1 3PJ, UK. E-mail: jin-chong.tan@eng.ox.ac.uk*

[b] *ISIS Facility, STFC Rutherford Appleton Laboratory, Chilton, Didcot OX11 0QX, UK*

† Electronic supplementary information (ESI) available: Materials synthesis methods, materials characterization techniques, INS spectra, electron micrographs, adsorption isotherms, TGA and FTIR spectra. See DOI: 10.1039/c8cc10089f

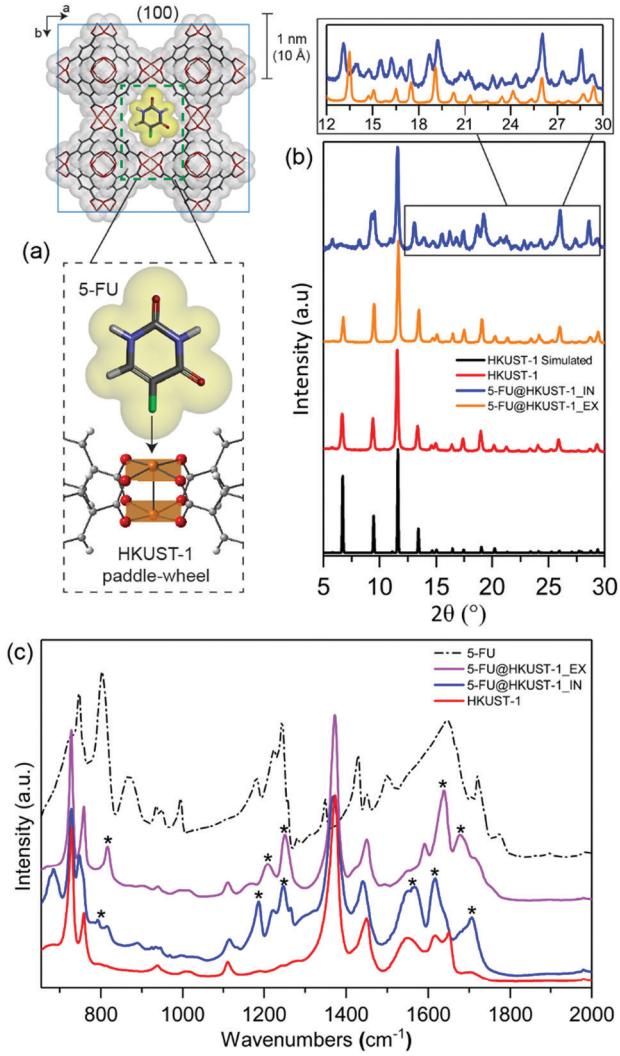

Fig. 1 Structural characterization of HKUST-1 and drug@MOF composites. (a) Schematic representation of guest–host interaction of 5-FU to the unsaturated metal sites located at the pore apertures of HKUST-1. Colour scheme: copper in orange, carbon in grey, oxygen in red, hydrogen in white, nitrogen in purple, and fluorine in green. (b) PXRD patterns of manually ground HKUST-1 and its drug-loaded counterparts. Inset shows the additional diffraction peaks emerging in 5-FU@HKUST-1_IN, compared to 5-FU@HKUST-1_EX. (c) FTIR spectra of HKUST-1 samples measured in ATR mode. Asterisks mark the position of the 5-FU peaks.

Bragg peaks of 5-FU@HKUST-1_EX match those of the pristine HKUST-1, the diffraction pattern of 5-FU@HKUST-1_IN is considerably different. It can be seen in Fig. 1b that the PXRD pattern of 5-FU@HKUST-1_IN exhibits some of the major peaks of HKUST-1 (albeit shifted), and appearance of several new diffraction peaks. These changes in diffraction pattern suggest that there is deformation to the host framework, causing the formation of a distorted phase of HKUST-1 with reduced symmetry. We hypothesize that the successful confinement of 5-FU drug molecules within the HKUST-1 pore *via* the *in situ* encapsulation strategy could give rise to structural distortions of the HKUST-1 unit cell. The coordination of the guest molecule to the CUS also affected the colour of the samples and its nominal density, as summarised in Fig. S1 (ESI†). Interestingly, we have established that the cubic structure of HKUST-1 is recoverable upon release of encapsulated guest from the 5-FU@HKUST-1_IN composite (Fig. S2, ESI†), evidenced from the emergence of Bragg peaks matching the pristine structure of HKUST-1. This recovery was also accompanied by the return of the characteristic colour shift of HKUST-1 upon activation, indicating the change in the copper coordination after guest release. On the other hand, 5-FU@HKUST-1_EX maintains its crystal integrity after release of 5-FU, showing no detectable structural changes (Fig. S3, ESI†). Importantly, the release of the guest can be confirmed by tracking the disappearance of the 5-FU peak in the attenuated total reflectance Fourier transform infrared (ATR-FTIR) spectra. 5-FU@HKUST-1_EX shows a nearly perfect recovery (Fig. S4, ESI†) towards the pristine HKUST-1, whereas 5-FU@HKUST-1_IN is less complete in 1500–1700 cm^{-1} (Fig. S5, ESI†) indicating a stronger guest–host interaction. Complete details of the guest release protocol can be found in ESI.†

The level of guest encapsulation was evaluated by Brunauer–Emmett–Teller (BET) surface area determination (Fig. S6, ESI†) and quantified by thermogravimetric analysis (TGA) (Fig. S7, ESI†). The surface area of the pristine HKUST-1 (1068 $m^2\ g^{-1}$) is in agreement with the values of other reported HKUST-1 samples synthesized by mechanochemistry (Table S2, ESI†).[4b–d] We have determined the drug loading in 5-FU@HKUST-1_IN and 5-FU@HKUST-1_EX to be 6.9 ± 0.8 wt% and 10.7 ± 1.4 wt%, respectively. The BET surface area of the samples was found to be greatly reduced to 13 $m^2\ g^{-1}$ and 463 $m^2\ g^{-1}$, respectively. Scanning Electron Microscopy (SEM) and Atomic Force Microscopy (AFM) images are presented in Fig. S8 (ESI†). The AFM topography shows the crystal morphology while SEM images display no sign of major alterations before and after drug encapsulation. The particle size was found to be 432 ± 83 nm.

In the ATR-FTIR spectra (Fig. 1c) the characteristic bands of HKUST-1 were detected in all samples (Table S3, ESI†), confirming the retention of the chemical bond integrity upon 5-FU loading. The spectra of 5-FU@HKUST-1_IN and 5-FU@HKUST-1_EX exhibit clear changes in the regions of 1100–1300 cm^{-1} and 1500–1700 cm^{-1}, in comparison to the pristine HKUST-1 spectrum. These modes originate from the stretching of –C–N and –C–F bonds of 5-FU,[14] corroborating the presence of drug molecules in the measured samples. However, there are salient differences between spectra of the two different drug-loaded composites: *in situ vs. ex situ*. Differences in the vibrational modes of the composites suggest the specific interactions between 5-FU and HKUST-1, due to guest confined inside the pore *versus* guest adsorbed outside the host framework.

Examination and comparison of the low energy vibrational bands, termed the terahertz (THz) modes of the *in situ* and *ex situ* derived composite samples, will offer additional insights into the different drug–MOF interactions. Unlike high frequency vibrations (Fig. 1c), arising from molecular vibrations of small functional groups, the low energy bands (from phonons) are observed in the lower frequency THz region. THz vibrations are collective modes associated with the lattice dynamics of the framework structure.[15] Using INS, it is possible to measure the

full vibrational spectrum[8] to reveal how the presence of the drug molecule affects THz dynamics of the host framework. Fig. 2 presents the experimental and theoretical INS spectra of HKUST-1 as well as its drug-loaded counterparts up to ~15 THz (500 cm^{-1}); the full spectra up to ~60 THz (2000 cm^{-1}) are shown in Fig. S9 and S10 (ESI†). Because identification of the origin of the THz vibrations is challenging, we employed the results from *ab initio* density functional theory (DFT) calculations recently reported by some of us,[16] to compute the theoretical INS spectrum of HKUST-1. This enables us to perform the assignment of the peaks observed in the experimental INS data. A reasonably good agreement between theory and experiments is observed in Fig. 2a. The THz modes in HKUST-1 can be divided into three regions: (I) below 4.5 THz (<150 cm^{-1}), associated with paddle-wheel deformation and translational motions; (II) 4.5–9 THz (~150–300 cm^{-1}), which contains asymmetric paddle-wheel deformation with Cu–Cu bond buckling and O–Cu–O bending modes; and (III) 9–18 THz (~300–600 cm^{-1}) exhibiting in-plane and out-of-plane deformations of aromatic rings. Herein the vibrational modes were designated as no. 1–19 (see Fig. 2a and Fig. S11, ESI†) to facilitate band identification; descriptions of all modes are given in Table S4 (ESI†).

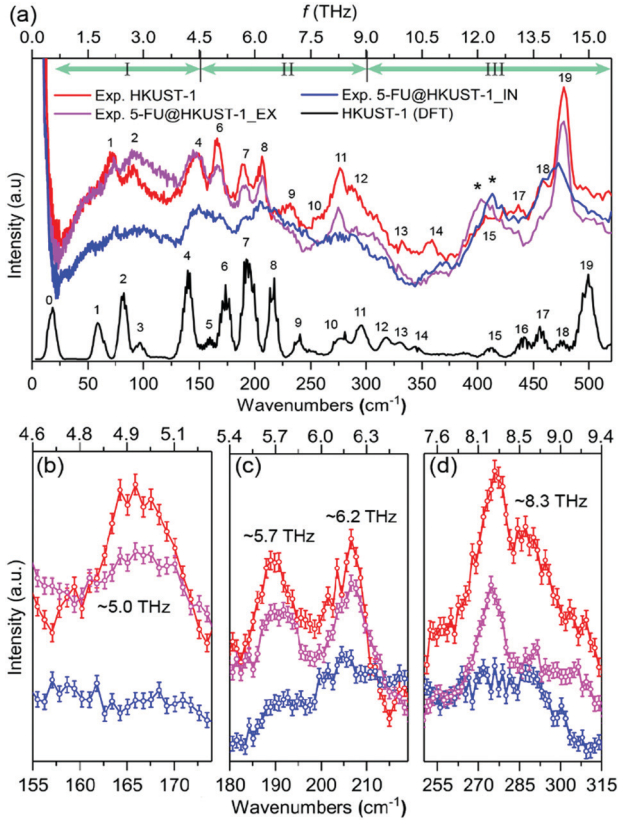

Fig. 2 (a) Comparison of experimental and theoretical inelastic neutron scattering (INS) spectra of HKUST-1 and its drug-loaded counterparts. The theoretical spectrum was calculated using our published DFT calculations.[16] Closer look at THz modes at (b) ~5.0 THz, (c) ~5.7 THz and ~6.2 THz, and (d) ~8.3 THz, whose lattice dynamics are illustrated in Fig. 3(a–d), respectively. Asterisks mark the positions of the 5-FU peaks. (1 THz ≈ 33.36 cm^{-1} ≈ 4.14 meV).

In region-I, an overall decrease in the intensity of the inelastic spectrum of 5-FU@HKUST-1_IN was detected. On TOSCA, INS spectrum intensity at low frequency (*i.e.* low momentum transfer (Q)) is proportional to the mean square displacement of the atoms from their equilibrium position, while at higher frequency the intensity is suppressed by the Debye–Waller factor.[17] On this basis, the decline of the spectral intensity in this sample may be explained by suppression of specific lattice modes, linked to strong guest–host interactions causing the framework distortions detected in the PXRD data (Fig. 1a). However, inelastic scattering of the 5-FU@HKUST-1_EX sample shows a different behavior. The relatively higher scattering intensity observed in the spectrum of this sample, specifically in the range of ~2.2–3.7 THz (74–125 cm^{-1}) might be a combination of scattering coming from the framework and the drug molecules, which indicates a weaker guest–host interaction. Likewise, a closer comparison between the spectra of 5-FU@HKUST-1_EX and 5-FU@HKUST-1_IN reveals a lower scattering intensity of the latter up to 6.4 THz (~213 cm^{-1}), accompanied by reduced integrated area under the inelastic spectrum.

Within region-II, we have pinpointed four THz modes that are most sensitive to 5-FU loading. Differences in the relative scattering intensity of the peaks at ~5.0 THz (166 cm^{-1}), ~5.7 THz (190 cm^{-1}), and ~6.2 THz (207 cm^{-1}), are observed in the spectra of drug-loaded samples (Fig. 2). These modes are, respectively, associated with paddle-wheel translational motion, asymmetric paddle-wheel deformation with Cu–Cu buckling and O–Cu–O bending accompanied by rocking mode of the organic linkers, whose vibrations are illustrated in Fig. 3. The decline in scattering intensity of these modes upon incorporation of 5-FU, see Fig. 2b and c, is accompanied by not only the reduction of the integrated area under the inelastic spectra (Table S5, ESI†), but also the significant broadening of these peaks in the *in situ* derived sample. The broadening was approximated by values of full width at half maximum (FWHM in Fig. S12, ESI†), which reflect the changes in vibrations of the aforementioned collective modes.

Data in Fig. 2d show suppression of the paddle-wheel vibrational modes in 5-FU@HKUST-1_IN, especially the peak at ~8.3 THz (276 cm^{-1}) attributed to asymmetric paddle-wheel deformation (O–Cu–O bending and Cu–Cu buckling). It can be seen that this mode completely vanishes upon the incorporation of 5-FU. We propose that confinement of 5-FU molecules within the distorted host framework is responsible for the suppression of vibrational modes observed here. Suppression of this mode indicates a change in the coordination environment of the copper paddle-wheel that also affects the deformation of the organic linker. The fall in the THz intensity could be correlated to hindrance of the paddle-wheel motions, due to interaction with drug molecules positioned inside (bound to CUS) or outside the pores of the framework (hydrogen bonded); herein the *in situ* confinement approach led to a greater decline of mode intensity than the *ex situ* method.

Turning to region-III, unambiguously, the new mode observed at ~12 THz (410 cm^{-1}) indicates the presence of 5-FU in the measured samples (Fig. S10 inset, ESI†), as previously detected in the ATR-FTIR data (Fig. 1c). The BTC linker deformation (~474–478 cm^{-1})

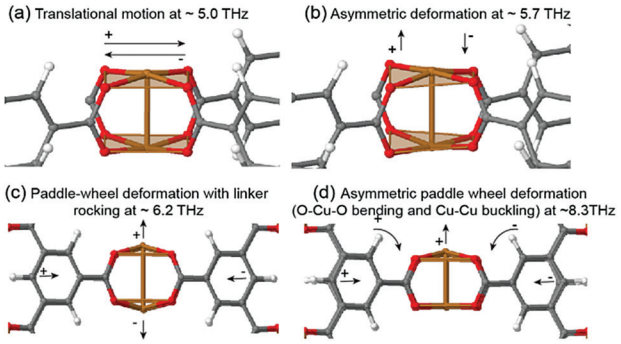

Fig. 3 Terahertz modes of HKUST-1 most affected by the presence of 5-FU guest, showing collective vibrations at (a) ~5.0 THz, (b) ~5.7 THz, (c) ~6.2 THz, and (d) ~8.3 THz. Arrows indicate the directions of the collective deformations with +/− amplitudes computed by DFT. Colour scheme: copper in orange, carbon in grey, oxygen in red, hydrogen in white.

has also been identified. The broadening of the peak attributed to organic linker vibrations reveals that framework distortion is not restricted to the CUS centers, but also affecting the walls of the cages comprising bridging organic linkers. Interestingly, the previously described modal changes are accompanied by smaller changes in the characteristic vibrational modes of the frameworks in the higher energy region of ~950–1500 cm^{-1}, see Fig. S10 (ESI†). Notable changes detected in the THz vibrations reveal the stronger guest–host intermolecular interactions present in the *in situ* derived samples, attributable to the confinement of 5-FU in the pores of HKUST-1 *via* coordination to the copper paddle-wheel. In contrast, during *ex situ* encapsulation, the drug molecules in solution will have to compete against the polar solvent for coordination to the active site and suffer from reduction in mobility from solvation effects. Consequently, the solvent molecules occupy some of the metallic active sites, thereby reducing the free binding sites available to drug molecules. Finally, propensity of forming hydrogen bonds with the external surface of the cages means that in the *ex situ* strategy the drug molecule has a higher likelihood to bind to framework exterior.

In summary, we have demonstrated that high-resolution inelastic neutron scattering spectroscopy offers new opportunities to study drug@MOF interactions, and more generally the guest@MOF confinement effects from a vibrational point of view. We have observed modifications in the THz lattice dynamics of 5-FU@HKUST-1_IN, where a sharp reduction in the low-energy collective modes under ~7.5 THz (250 cm^{-1}) marks the suppression of the copper paddle-wheel motions due to drug incorporation. By leveraging the mechanochemical method, we show that an *in situ* one-pot strategy can directly encapsulate molecules into the pores of the host framework. The *in situ* drug encapsulation methodology may have the potential to minimize the burst effect,[11] contributing to the development of improved pathways to control the binding and release of drug molecules from MOFs.

B. E. S. thanks the Minas Gerais Research Foundation (FAPEMIG CNPJ n21.949.888/0001-83) for a DPhil scholarship award. J. C. T. thanks the ERC Consolidator Grant under the grant agreement 771575 (PROMOFS). The INS experiments were performed at ISIS Neutron and Muon Source on the TOSCA spectrometer through beamtime award RB1810348. We thank the Research Complex at Harwell (RCaH) for access to the TGA-Q50 and the Nicolet iS10 FTIR spectrometer.

Conflicts of interest

There are no conflicts to declare.

Notes and references

1 (*a*) A. C. McKinlay, R. E. Morris, P. Horcajada, G. Ferey, R. Gref, P. Couvreur and C. Serre, *Angew. Chem., Int. Ed.*, 2010, **49**, 6260–6266; (*b*) Y. Li, X. Li, Q. Guan, C. Zhang, T. Xu, Y. Dong, X. Bai and W. Zhang, *Int. J. Nanomed.*, 2017, **12**, 1465–1474; (*c*) J. Xiao, Y. Zhu, S. Huddleston, P. Li, B. Xiao, O. K. Farha and G. A. Ameer, *ACS Nano*, 2018, **12**, 1023–1032.
2 (*a*) J. Jiang, Y. Zhao and O. M. Yaghi, *J. Am. Chem. Soc.*, 2016, **138**, 3255–3265; (*b*) B. Supronowicz, A. Mavrandonakis and T. Heine, *J. Phys. Chem. C*, 2015, **119**, 3024–3032.
3 S. L. James, C. J. Adams, C. Bolm, D. Braga, P. Collier, T. Friscic, F. Grepioni, K. D. M. Harris, G. Hyett, W. Jones, A. Krebs, J. Mack, L. Maini, A. G. Orpen, I. P. Parkin, W. C. Shearouse, J. W. Steed and D. C. Waddell, *Chem. Soc. Rev.*, 2012, **41**, 413–447.
4 (*a*) D. Crawford, J. Casaban, R. Haydon, N. Giri, T. McNally and S. L. James, *Chem. Sci.*, 2015, **6**, 1645–1649; (*b*) J. Yang, X. Feng, G. Lu, Y. Li, C. Mao, Z. Wen and W. Yuan, *Dalton Trans.*, 2018, **47**, 5065–5071; (*c*) M. Samal, J. Panda, B. P. Biswal and R. Sahu, *CrystEngComm*, 2018, **20**, 2486–2490; (*d*) M. Klimakow, P. Klobes, A. F. Thünemann, K. Rademann and F. Emmerling, *Chem. Mater.*, 2010, **22**, 5216–5221.
5 (*a*) R. Babarao and J. W. Jiang, *J. Phys. Chem. C*, 2009, **113**, 18287–18291; (*b*) P. Horcajada, C. Serre, G. Maurin, N. A. Ramsahye, F. Balas, M. Vallet-Regi, M. Sebban, F. Taulelle and G. Ferey, *J. Am. Chem. Soc.*, 2008, **130**, 6774–6780.
6 (*a*) M. Kondo, T. Yoshitomi, K. Seki, H. Matsuzaka and S. Kitagawa, *Angew. Chem., Int. Ed.*, 1997, **36**, 1725–1727; (*b*) D. Venkataraman, G. B. Gardner, S. Lee and J. S. Moore, *J. Am. Chem. Soc.*, 1995, **117**, 11600–11601; (*c*) O. M. Yaghi, G. M. Li and H. L. Li, *Nature*, 1995, **378**, 703–706.
7 K. Xing, R. Fan, F. Wang, H. Nie, X. Du, S. Gai, P. Wang and Y. Yang, *ACS Appl. Mater. Interfaces*, 2018, **10**, 22746–22756.
8 *Neutron Scattering – Fundamentals, Experimental Methods in the Physical Sciences*, ed. F. Fernandez-Alonso and D. L. Price, Academic Press, New York, 2013.
9 (*a*) J. Eckert, *Spectrochim. Acta, Part A*, 1992, **48**, 271–283; (*b*) M. E. Casco, Y. Q. Cheng, L. L. Daemen, D. Fairen-Jimenez, E. V. Ramos-Fernandez, A. J. Ramirez-Cuesta and J. Silvestre-Albero, *Chem. Commun.*, 2016, **52**, 3639–3642.
10 (*a*) S. F. Parker, F. Fernandez-Alonso, A. J. Ramirez-Cuesta, J. Tomkinson, S. Rudic, R. S. Pinna, G. Gorini and J. Fernández Castañon, *J. Phys.: Conf. Ser.*, 2014, **554**, 012003; (*b*) R. S. Pinna, S. Rudić, S. F. Parker, J. Armstrong, M. Zanetti, G. Škoro, S. P. Waller, D. Zacek, C. A. Smith, M. J. Capstick, D. J. McPhail, D. E. Pooley, G. D. Howells, G. Gorini and F. Fernandez-Alonso, *Nucl. Instrum. Methods Phys. Res., Sect. A*, 2018, **896**, 68–74.
11 X. Huang and C. S. Brazel, *J. Controlled Release*, 2001, **73**, 121–136.
12 A. A. Talin, A. Centrone, A. C. Ford, M. E. Foster, V. Stavila, P. Haney, R. A. Kinney, V. Szalai, F. El Gabaly, H. P. Yoon, F. Leonard and M. D. Allendorf, *Science*, 2014, **343**, 66–69.
13 R. Anand, F. Borghi, F. Manoli, I. Manet, V. Agostoni, P. Reschiglian, R. Gref and S. Monti, *J. Phys. Chem. B*, 2014, **118**, 8532–8539.
14 V. K. Rastogi and M. A. Palafox, *Spectrochim. Acta, Part A*, 2011, **79**, 970–977.
15 M. R. Ryder, B. Civalleri, T. D. Bennett, S. Henke, S. Rudic, G. Cinque, F. Fernandez-Alonso and J. C. Tan, *Phys. Rev. Lett.*, 2014, **113**, 215502.
16 M. R. Ryder, B. Civalleri, G. Cinque and J.-C. Tan, *CrystEngComm*, 2016, **18**, 4303–4312.
17 A. Griffin and H. Jobic, *J. Chem. Phys.*, 1981, **75**, 5940–5943.